Supplementary materials for

A new nanocrystalline inorganic-organic hybrid exhibiting semiconductor properties and applications

Haijuan Du, Wenli Zhang, Chaohai Wang, Yunyin Niu,* and Hongwei Hou*

College of Chemistry and Molecular Engineering, Zhengzhou University, Zhengzhou 450001, P. R. China. *E-mail: niuyy@zzu.edu.cn, houhongw@zzu.edu.cn*

Experimental

Materials and methods

The cation benzyl viologen (BV^{2+}) was synthesized according to the reported literature method.[1] Other chemicals were of reagent grade and used as purchased without further purification. The IR spectrum was recorded on a Shimazu IR435 spectrometer as KBr disk (4000–400 cm^{-1}). Elemental analysis (C, H, and N) was carried out on a FLASH EA 1112 elemental analyzer. The purity of the bulk microcrystalline materials obtained from the syntheses was checked by Powder X-ray diffraction analysis. Powder X-ray diffraction (PXRD) pattern was recorded using Cu Kα1 radiation on a PAN analytical X'Pert PRO diffractometer. Thermogravimetric analysis (TGA) was carried out on a model NETZSCHTG209 thermal analyzer in flowing N_2 atmosphere of 20 $mL \cdot min^{-1}$ at a heating rate of 10 $°C \cdot min^{-1}$ in the temperature range 0-800 °C using platinum crucibles. The UV-Vis diffuse reflectance spectrum (DRS) was recorded on a Cary 5000 UV-Vis-NIR at the speed of 300 nm min^{-1} from 800 to 200 nm. UV-Vis absorption spectra were obtained using UV-5500 PC spectrophotometer. Fluorescence spectrum was carried out with a FL-7000 spectrometer and the lifetime was performed on Edinburgh FL980. The morphology of the crystalline sample was observed on Tecnai G2F20 transmission electron microscope (FEI) at the accelerating voltage of 200 kv. The dielectric property was measured at ambient temperature using PNA-N5244A spectrometer (Agilent Technologies Co. Ltd.) from 2 to18GHz. The XPS spectrum was recorded on a multipurpose X-ray photoelectron spectroscope (Thermo ESCALAB 250Xi,

America) with a microfocused monochromatic X-ray source of Al Kα, using adventitious carbon (C1s 284.8 eV) as the calibration reference. Electrochemical measurements were performed with a RST5000 electrochemical workstation. A Ag/AgCl electrode was used as a reference electrode, and a Pt wire as a counter electrode. Chemically bulk-modified carbon-paste electrode (CPE) was used as the working electrode.

Compound synthesis

A methanol solution of [BV]·2Br (26.0 mg, 0.05 mmol) was added into a stirring solution of AgBr (9.4 mg, 0.05 mmol) with the presence of excessive KBr (0.40-0.45 mmol) dissolved in N, N- dimethylformamide (DMF). More DMF, otherwise more methanol, is needed if precipitation appears until the precipitation almost disappeared. The clear solution filtrated is to be slowly evaporated in a vial at ambient temperature and several days later yellow crystals suitable to X-ray diffraction, $[(BV)_2(Ag_5Br_9)]_n$, were obtained in yield of 54% based on silver ions. Anal. calcd (%) for **1**: C, 29.79; H, 2.30; N, 2.90. Found: C, 29.72; H, 2.32; N, 2.93. IR (KBr, cm^{-1}): 3442(s), 3050(w), 1631(m), 1556(m), 1492(m), 1435(m), 1348(w), 1257(w), 1207(w), 1144(m), 1041(w), 1026(w), 931(w), 837(w), 802(w), 786(w), 744(m), 703(m), 622(w), 558(w), 458(w).

Preparation of CPE. The carbon paste electrode bulk-modifed with compound **1** (**1**-CPE) was fabricated as follows: 0.1 g of compound **1** and 0.5 g of graphite powder were mixed and grounded together by an agate mortar and pestle to achieve a uniform mixture, and then 0.05 mL of liquid paraffin was added with stirring. The homogenized mixture was packed into a glass tube with a 3 mm inner diameter, and the tube surface was wiped with weighing paper. Electrical contact was established with a copper rod through the back of the electrode.

X-ray crystallography study

Crystallographic data for the compound was collected at 100(2)K on a Bruker APEX-II area-detector diffractometer equipped with graphite-monochromatized Mo-Ka radiation (λ = 0.71073Å). Its structure was solved by direct method and expanded using Fourier techniques. The non-hydrogen atoms were refined with anisotropic

thermal parameters. The hydrogen atoms were assigned with common isotropic displacement factors and included in the final refinement by using geometrical constraint. The structure was refined with full-matrix least-squares techniques on F^2 using the OLEX-2 program package.[2] Crystal data for **1** was summarized in detail in Table S1. Selected bond lengths and bond angles were put in Table S2.

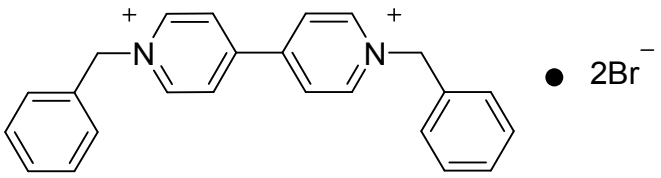

Scheme 1

Table S1 Crystal data and structure refinement details for **1**.

	1
formula	$C_{48}H_{44}Ag_5Br_9N_4$
formula weight	1935.41
crystal system	Triclinic
space group	*P*-1
a/Å	10.4312(4)
b/Å	11.1981(8)
c/Å	13.2196(10)
α/deg	73.325(6)
β/ deg	78.580(6)
γ/ deg	66.409(6)
vol/Å^3	1349.53(17)
Z	1
D_c/g cm^{-3}	2.381
μ/mm^{-1}	8.481
F(000)	910.0
rflns collected	11957
unique rflns	6172
GOF	1.032
R_1[a] ($I > 2\acute{o}(I)$)	0.0431
wR_2[a] (all data)	0.0976
$\Delta\rho$max/$\Delta\rho$min(e^{-3})	1.37/-1.36

[a] $R_1 = ||Fo| - |Fc||/ |Fo|$; $wR_2 = [w(Fo^2 - Fc^2)^2/ w(Fo^2)^2]^{1/2}$

Table S2. Selected bond distances(Å) and angles(°)for compound **1**.

Compound 1					
Ag(1)-Ag(2)	3.3405(7)	Ag(1)-Ag(3)	3.1721(19)	Ag(1)-Ag(3)^3	3.1785(19)
Ag(1)-Br(1)	2.5695(7)	Ag(1)-Br(2)	2.7069(8)	Ag(1)-Br(3)^3	2.8294(7)
Ag(1)-Br(5)	2.7462(8)	Ag(2)-Ag(3)^3	3.189(2)	Ag(2)-Ag(3)	3.1441(19)
Ag(2)-Br(2)	2.6878(8)	Ag(2)-Br(3)	2.7907(7)	Ag(2)-Br(4)	2.6166(5)
Ag(2)-Br(5)	2.7118(8)	Ag(3)-Ag(1)^3	3.1786(19)	Ag(3)-Ag(2)^3	3.189(2)
Ag(3)-Br(3)	2.6315(18)	Ag(3)-Br(3)^3	2.6287(18)		
Br(3)-Ag(1)^3	2.8295(7)	Br(3)-Ag(3)^3	2.6288(18)	Br(4)-Ag(2)^4	2.6166(5)
Ag(3)^3-Ag(1)-Ag(2)	58.50(4)	Ag(3)-Ag(1)-Ag(2)	57.66(3)	Ag(3)-Ag(1)-Ag(3)^3	16.93(4)
Br(1)-Ag(1)-Ag(2)	147.34(2)	Br(1)-Ag(1)-Ag(3)^3	152.50(4)	Br(1)-Ag(1)-Br(2)	123.80(3)
Br(1)-Ag(1)-Br(3)^3	103.95(2)	Br(1)-Ag(1)-Br(5)	120.27(2)	Br(2)-Ag(1)-Ag(2)	51.484(17)
Br(2)-Ag(1)-Ag(3)^3	77.42(3)	Br(2)-Ag(1)-Ag(3)	62.90(3)	Br(2)-Ag(1)-Br(3)^3	99.29(2)
Br(2)-Ag(1)-Br(5)	103.26(2)	Br(3)^3-Ag(1)-Ag(2)	108.70(2)	Br(3)^3-Ag(1)-Ag(3)	51.57(4)
Br(3)^3-Ag(1)- Ag(3)^3	51.55(4)	Br(5)-Ag(1)-Ag(2)	51.798(18)	Br(5)-Ag(1)-Ag(3)	76.58(3)
Br(5)-Ag(1)- Ag(3)^3	62.90(3)	Br(5)-Ag(1)-Br(3)^3	102.07(3)	Ag(3)^3-Ag(2)-Ag(1)	58.21(3)
Ag(3)-Ag(2)-Ag(1)	58.48(3)	Ag(3)-Ag(2)-Ag(3)^3	16.96(4)	Br(2)-Ag(2)-Ag(1)	51.999(18)
Br(2)-Ag(2)-Ag(3)	63.49(3)	Br(2)-Ag(2)-Ag(3)^3	77.50(3)	Br(2)-Ag(2)-Br(3)	103.07(2)
Br(2)-Ag(2)-Br(5)	104.70(2)	Br(3)-Ag(2)-Ag(1)	109.34(2)	Br(3)-Ag(2)-Ag(3)^3	51.64(3)
Br(3)-Ag(2)-Ag(3)	52.23(4)	Br(4)-Ag(2)-Ag(1)	147.60(2)	Br(4)-Ag(2)-Ag(3)	150.85(3)
Br(4)-Ag(2)-Ag(3)^3	154.18(4)	Br(4)-Ag(2)-Br(2)	117.30(2)	Br(4)-Ag(2)-Br(3)	102.87(2)
Br(4)-Ag(2)-Br(5)	126.06(2)	Br(5)-Ag(2)-Ag(1)	52.732(18)	Br(5)-Ag(2)-Ag(3)	77.54(3)
Br(5)-Ag(2)-Ag(3)^3	63.08(3)	Br(5)-Ag(2)-Br(3)	98.64(3)	Ag(1)-Ag(3)-Ag(1)^3	163.07(4)
Ag(1)-Ag(3)-Ag(2)^3	113.16(5)	Ag(1)^3-Ag(3)-Ag(2)^3	63.29(4)	Ag(2)-Ag(3)-Ag(1)	63.86(4)
Ag(2)-Ag(3)-Ag(1)^3	114.21(5)	Ag(2)-Ag(3)-Ag(2)^3	163.04(4)	Ag(3)^3-Ag(3)-Ag(1)^3	81.1(2)
Ag(3)^3-Ag(3)-Ag(1)	81.9(2)	Ag(3)^3-Ag(3)-Ag(2)	84.2(2)	Ag(3)^3-Ag(3)-Ag(2)^3	78.8(2)
Ag(3)^3-Ag(3)-Br(3)^3	79.9(2)	Ag(3)^3-Ag(3)-Br(3)	79.6(2)	Br(3)-Ag(3)-Ag(1)	57.48(4)
Br(3)-Ag(3)-Ag(1)^3	57.36(4)	Br(3)^3-Ag(3)-Ag(1)^3	119.02(7)	Br(3)^3-Ag(3)-Ag(2)^3	56.35(4)
Br(3)-Ag(3)-Ag(2)^3	118.99(6)	Br(3)^3-Ag(3)-Ag(2)	120.66(6)	Br(3)-Ag(3)-Ag(2)	56.96(4)
Br(3)^3-Ag(3)-Br(3)	159.53(5)				

Symmetric code: ^{1}1-x,-y,-z; ^{2}-x,1-y,1-z; ^{3}1-x,-y,1-z; ^{4}1-x,1-y,1-z

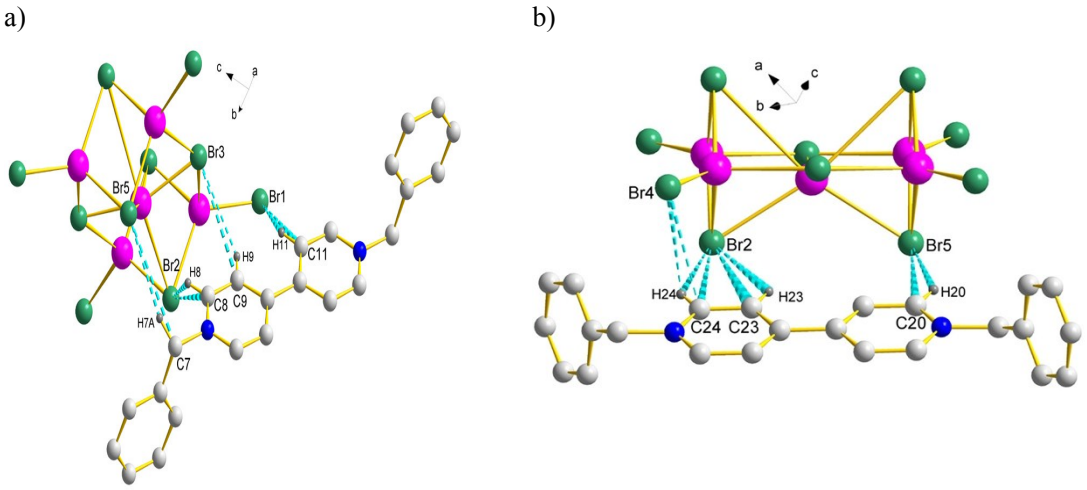

Fig.S1 a) a view of C8-H8···Br2, C11-H11···Br1, C9-H9···Br3 and C7-H7A···Br5 hydrogen bonds of compound **1**. **b**) a view of C24-H24···Br2, C20-H20···Br5, C23-H23···Br2 and C24-H24···Br4 hydrogen bonds of compound **1**.

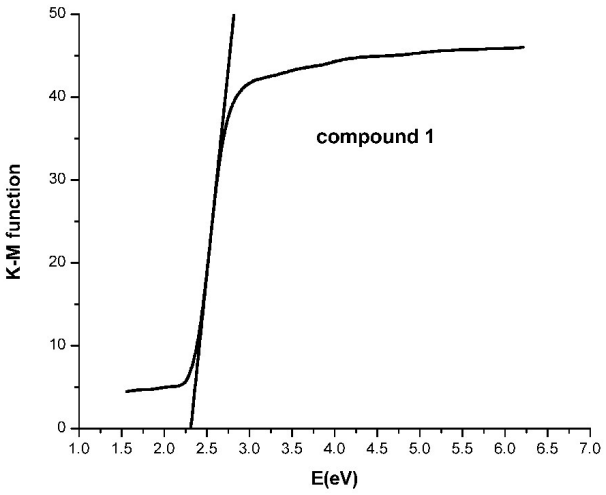

Fig. S2 K-M function versus energy (eV) curve compound **1**.

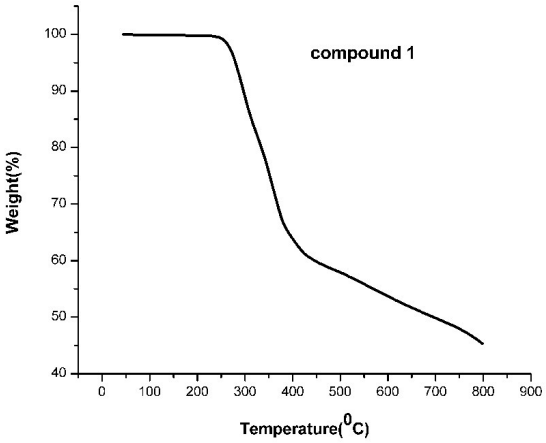

Fig. S3 TG plot of compound **1.**

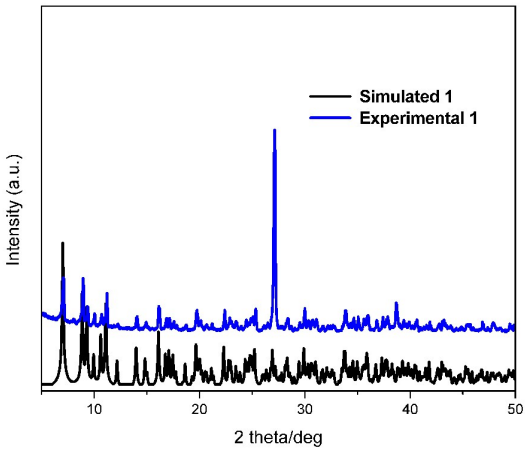

Fig. S4. Powder X-ray diffraction (PXRD) patterns for **1**. Blue: experimental data ; black: simulated pattern from single-crystal X-ray structure data.

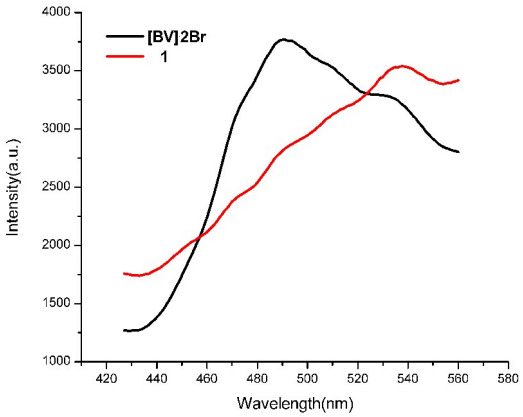

Fig. S5. Solid-state photoluminescent spectrum of **1** and corresponding cation at room temperature.

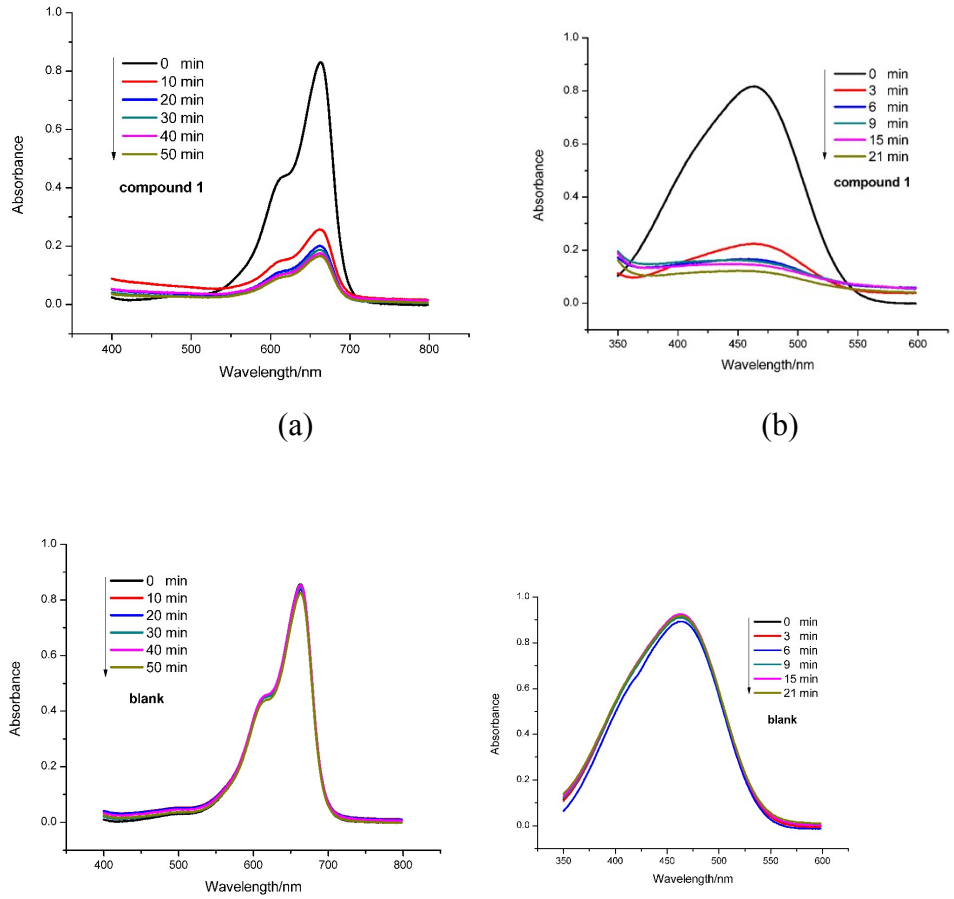

Fig.S6 Absorption spectra of the MB aqueous solution during the adsorption process with the use of compound **1** (a) and **blank** (c). Absorption spectra of the MO aqueous solution during the adsorption process with the use of compound **1** (b) and **blank** (d).

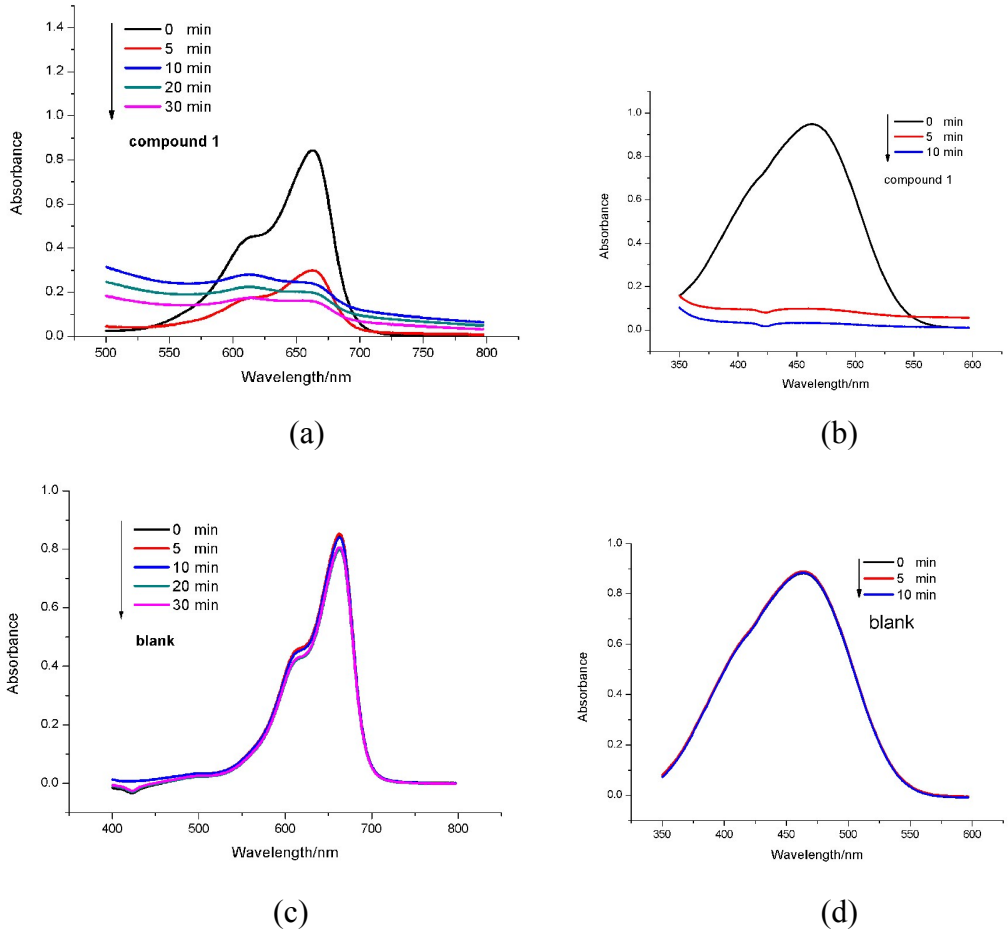

Fig.S7 Absorption spectra of the MB aqueous solution during the photocatalytic decomposition reaction with the use of compound **1** (a) and **blank** (c). Absorption spectra of the MO aqueous solution during the photocatalytic decomposition reaction with the use of compound **1** (b) and **blank** (d).

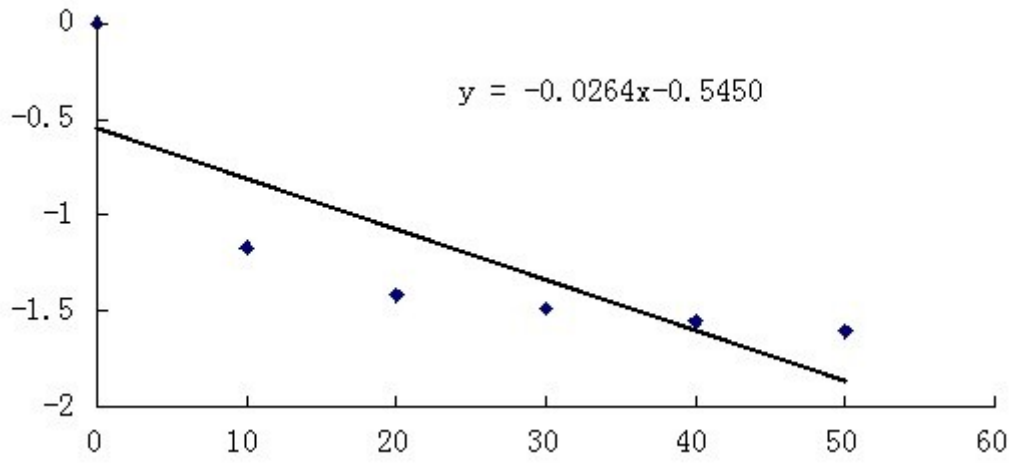

Fig. S8 Ln(C/C_0) versus time plot with the use of compound **1** treated MB solution.

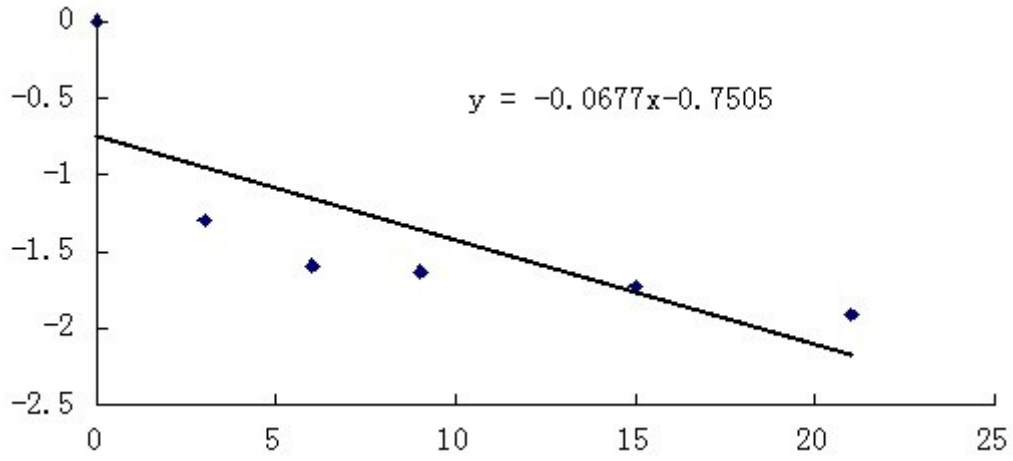

Fig. S9 Ln(C/C_0) versus time plot with the use of compound **1** treated MO solution.

1 T. Higashi and T. Sagara, *Electrochimica Acta*, 2013, **114**, 105.

2 O. V. Dolomanov, L. J. Bourhis, R. J. Gildea, J. A. K. Howard and H. Puschmann, *J. Appl. Cryst.*, 2009, **42**, 339.